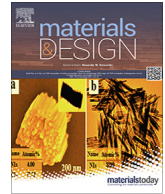


ULRR

An investigation of polyether Imide (PEI) toughening of carbon fibre-reinforced polyether ether ketone (PEEK) laminates

Item Type	Article
Authors	McLaughlin, John W.;Tobin, Emma;O'Higgins, Ronan M.
Citation	Materials & Design 212, 110189
Publisher	Elsevier
Download date	2026-04-12 11:32:08
Item License	https://creativecommons.org/licenses/by-nc-sa/1.0/
Link to Item	https://hdl.handle.net/10344/10750



An investigation of Polyether Imide (PEI) toughening of carbon fibre-reinforced Polyether Ether Ketone (PEEK) laminates

John W. McLaughlin, Emma Tobin, Ronan M. O'Higgins*

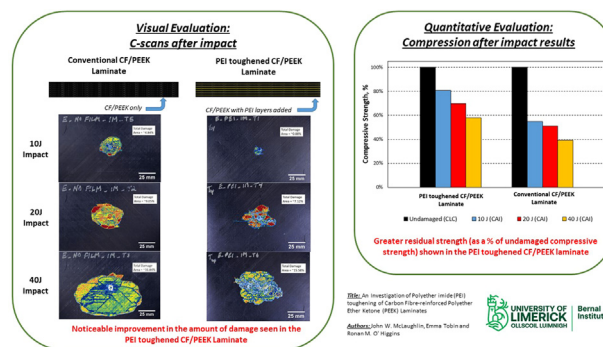
School of Engineering and Bernal Institute, University of Limerick, Ireland



HIGHLIGHTS

- PEI film inclusions improve the Mode I and Mode II interlaminar toughness performance of CF/PEEK laminates.
- CF/PEEK laminates toughened with PEI film at delamination susceptible ply interfaces exhibited superior impact performance relative to baseline CF/PEEK laminates.
- PEI film toughened CF/PEEK laminates exhibited a smaller impact damage footprint relative to baseline CF/PEEK laminates.
- Unlike thermoset based composite laminates, all CF/PEEK and PEI toughened CF/PEEK laminates tested exhibited impact damage on the impact surface. This is a useful attribute in aerospace structures, where barely visible impact damage (BVID) is a concern for flight safety.

GRAPHICAL ABSTRACT



ARTICLE INFO

Article history:

Received 13 July 2021

Revised 13 September 2021

Accepted 19 October 2021

Available online 21 October 2021

Keywords:

Thermoplastic composites

Impact

Vulnerability

Toughening

PEEK

PEI

ABSTRACT

Current thermoset composite material systems have relatively low interlaminar fracture toughness, leaving them vulnerable to impact damage. While thermoplastic based systems are considered to be tougher, toughness levels can be dependent on processing parameters. In this study, Polyether imide (PEI) film layers were added to carbon fibre-reinforced Polyether ether ketone (CF/PEEK) laminate layups prior to consolidation to enhance the interlaminar toughness at key ply interfaces. It was found that the addition of the PEI film improves the Mode I and Mode II interlaminar toughness of the laminate. Low-velocity impact tests were performed on the PEI toughened CF/PEEK laminates, as well as a baseline CF/PEEK laminate and a CF/PEEK laminate with PEEK film inserts, for direct laminate thickness comparison. For low energy impacts (10 J), associated with tool drop events, it was found that the PEI toughened panel performed best. However, the performance difference decreased as the impact energy increased. Ultrasonic scans indicated that PEI toughened CF/PEEK laminates exhibited a smaller damage footprint. Compression after impact (CAI) and Combined Loading Compression (CLC) tests revealed that although the PEI inserts reduce the laminate undamaged compressive strength, they exhibited higher relative residual strengths compared to the other laminates tested.

© 2021 The Authors. Published by Elsevier Ltd. This is an open access article under the CC BY-NC-ND license (<http://creativecommons.org/licenses/by-nc-nd/4.0/>).

* Corresponding author.

E-mail address: ronan.ohiggins@ul.ie (R.M. O'Higgins).

1. Introduction

With the requirement to produce more fuel efficient and environmentally friendly aircraft, fibre-reinforced polymer composites are finding increasing application in aircraft primary and secondary structures. However, composite laminates are more susceptible to impact damage than traditional metallic materials. Wenner and Drury [1] analysed the human error that resulted in damage to commercial aircraft while on the ground. Over this 39-month period, 265 incidents were reported, including tools, materials and work stands contacting the aircraft, unmanned equipment rolling into the aircraft and hangar doors closing on the aircraft. Composite laminate response to these types of impact events is a key design consideration. Composite laminates subjected to low-velocity impact (LVI) can sustain significant internal damage, with little evidence of damage apparent on the impact surface [2–4], often referred to as barely visible impact damage (BVID). The damage found after an impact may result in a significant reduction of the structures residual compression strength and stiffness. This type of damage can be characterised as a multi-part combination of interlaminar fracture (delamination), intralaminar fracture (transverse matrix cracking and debonding between fibre and matrix) and fibre fracture [5,6].

Polyether Ether Ketone (PEEK) is a semi-crystalline thermoplastic that has found application as a matrix in aerospace grade fibre-reinforced composite materials. Relative to thermoset based equivalents, carbon fibre-reinforced PEEK (CF/PEEK) is considered a tough composite. However, it has been shown that the degree of toughness and impact performance is dependent on the PEEK crystallinity [7–10]. PEEK crystallinity is highly dependent on the processing parameters. Ray et al. [9] and Comer et al. [10] showed that there was a significant variation in the crystallinity, and consequently interlaminar strength and toughness, for CF/PEEK processed by autoclave and laser-assisted automatic tape placement (LATP). Autoclave processed laminates, which experienced a relatively slow cooling rate, exhibited high crystallinity ($\approx 40\%$, close to crystallinity saturation), while the LATP processed laminate crystallinity was found to be relatively low ($\approx 15\text{--}20\%$) for laminates processed on a cold tool. However, as the tool temperature was increased, the laminate crystallinity was found to increase. Intralaminar properties were found to be best for high crystallinity laminates, as crystallinity seeded around the fibres providing good fibre/matrix interface bonding, but more brittle interlaminar performance. While low crystallinity laminates exhibited excellent interlinear toughness, but poorer intralaminar properties.

While the influence of processing parameters, in particular cooling rate, on the crystallinity levels in PEEK is relatively well understood, it is difficult to control processing parameters to achieve specific PEEK crystallinity in a laminate. Cooling rates can be defined that achieve relatively high or low levels of crystallinity. Most common processing methods (hot-press, stamping, autoclave etc.) yield relatively uniform crystallinity throughout the laminate. As a result, processing parameters are tuned to yield a laminate with a relatively high crystallinity ($\approx 33\%$), which provides good intralaminar properties, but less than optimal interlaminar toughness. This is generally deemed acceptable as CF/PEEK has significantly better interlaminar toughness relative to thermoset based materials. Post-consolidation processes such as hot-gas torch repress treatment [11] and laser repress treatment [12] have also been studied in the past as methods of improving the mechanical properties of CF/PEEK laminates, however neither method significantly increased the levels of the crystallinity.

Further methods of toughening PEEK composites have included the addition of a toughening medium. He et al. [13] created graphene oxide (GO) enhanced PEEK composites to be used for hard

tissue implant application, manufactured using injection moulding techniques. The study looked at the effect of GO loadings on the hybrid composite and found that a 0.5%GO-PEEK demonstrated a 127.2% greater energy absorption when compared to pure PEEK. Various studies have also shown that manipulating the coating applied to the surface of the carbon fibres (i.e. the sizing) can also have a positive effect on the interfacial shear strength (IFSS), which reflects the load transfer efficiency between the fibre and the resin, and the interlaminar shear strength (ILSS), which reflects the strength between the laminate planes, of a thermoplastic laminate [14–20]. Chen et al. [20] manufactured CF/PEEK prepregs that had PEI and GO sizing coated onto the fibres. These prepregs were then laid up in the unidirectional fibre orientation on a steel mould to prepare impregnated composites. The results of these impregnated CF/PEEK laminates showed an increase in 44% and 12% in the IFSS and ILSS data respectively. While the methods described above have resulted in large increases in the mechanical properties associated with toughness, it is desirable to find a toughening method that can be used on commercial CF/PEEK prepregs than can be used in traditional autoclave and pressforming manufacturing methods.

In this study, a method of improving CF/PEEK laminate interlaminar toughness is proposed, by inserting amorphous interlaminar layers between delamination susceptible plies. It has been shown that delamination of composite laminates during low-velocity impacts occurs between plies with a large angle difference [21–23]. This method allows laminates to be processed as normal to achieve relatively high intralaminar properties, by maximising in-ply PEEK crystallinity, but having a tough amorphous interlaminar region. To achieve this, amorphous polyether imide (PEI) films were inserted between specific plies in a CF/PEEK laminate stacking. PEI was chosen as the toughening material in this study for a number of reasons:

1. PEI is miscible with PEEK allowing both polymers to mix together to form a hybrid polymer. The glass transition temperature of PEEK is lower than that of PEI (138 °C and 217 °C respectively), resulting in the PEEK having a lower viscosity at high temperature, ensuring both thermoplastic materials mix [24].
2. PEI can withstand high temperatures, with the main decomposition step at 510 °C [25]. As the processing temperature for the CF/PEEK being used for this study is 390 °C, the properties of the PEI are not degraded as a result of consolidation [26].
3. PEI is amorphous [27], so the PEEK/PEI local polymer blend will have a lower crystallinity than PEEK. The lower crystallinity polymer at the ply interfaces should result in higher interlaminar fracture toughness [8].

Mode I and Mode II fracture toughness of CF/PEEK laminates with and without PEI inserts were characterised using double cantilevered beam (DCB) and end notch flexure (ENF) tests, respectively. While impact testing was carried out to assess the influence of PEI inserts on the damage tolerance and residual strength of CF/PEEK laminates. The additional PEI layers increased the thickness of the toughened panels and reduced their fibre volume fraction, potentially influencing the impact test results. To access the effect of the additional laminate thickness, CF/PEEK laminates with PEEK film inserts corresponding to the PEI insert locations were also tested.

PEI is sometimes used as a medium for adhering CF/PEEK components during co-consolidation or thermal fusion processes. To the authors' best knowledge, this is the first time that a study of this method for toughening CF/PEEK laminates has been documented in the open literature. The method has the advantage of neither requiring a significant alteration of conventional process-

ing methods nor requiring any secondary process to enhance the toughness of the CF/PEEK laminate.

2. Specimen manufacturing and characterisation

2.1. DCB specimens

Two CF/PEEK (Tenax®-E TPUD PEEK-2-34-IMS65 P12 24 K-UD-190) laminates were autoclave manufactured, each of a [0]₁₆ lay-up, with one panel having a PEI film inserted at the mid-plane. A strip of aluminium foil (~10 µm), coated in Frekote™ mould release, was placed at the mid-plane of each panel to act as a crack initiator. The foil was placed 40 mm into the laminate, perpendicular to the fibres (Fig. 1). Aluminium foil was used as it was the same thickness as Teflon film, usually used as a crack initiator insert, but is able to withstand the high temperature required for CF/PEEK consolidation. A slow cooling rate (2 °C/min) was used during the CF/PEEK panel consolidation, to induce a relatively high degree of crystallinity in the laminate, resulting in optimum intralaminar mechanical properties [28].

Laminates were cut to size in accordance with AITM 1.0005 [29], and aluminium tabs were adhered onto the specimens in order to facilitate the Mode I DCB tests (Fig. 1).

2.2. Impact testing specimens

All panels were laid up according to the laminate stacking sequences provided in Table 1. The stacking sequence is a zero-dominated lay-up based on an aircraft fuselage skin laminate designed to sustain high axial loads in compression/tension [30]. The CF/PEEK (Tenax®-E TPUD PEEK-2-34-IMS65 P12 24 K-UD-190) panels were laid up by hand and autoclave consolidated according to the supplier's instructions. For the ZD_PEI and ZD_PEEK panels (Table 1), the film inserts were Sabic ULTEM 1000B PEI film and Victrex APTIV® 2000 PEEK film, respectively. Both film inserts had a nominal thickness of 0.125 mm. Rectangular (100 mm × 150 mm) impact test panels were harvested from the consolidated laminates for impact testing according to ASTM D7136 [31]. The nominal fibre volume fraction of the ZD_NoFilm laminate was 66%. This value decreased to 57% and 56% for the ZD_PEI and ZD_PEEK laminates, respectively, due to the addition of the purely resin film inserts.

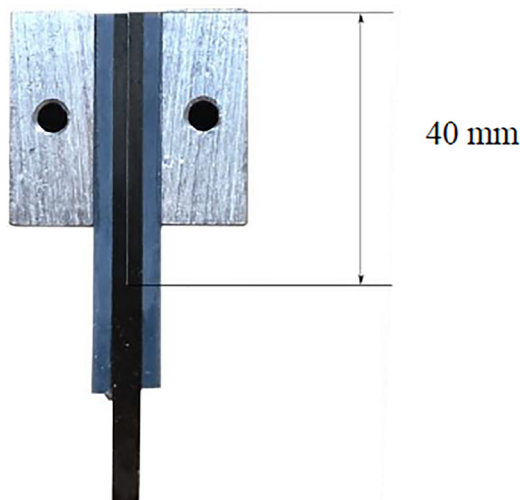


Fig. 1. Crack initiator placed within CF/PEEK specimens.

3. Experimentation

3.1. Interlaminar toughness of PEI toughened panels

3.1.1. Mode I interlaminar toughness

DCB tests were carried out in accordance with AITM 1.0005 [29] to determine the Mode I interlaminar toughness. Tests were carried out on a Tinius Olsen H25KS using a 1kN load cell. Five specimens of CF/PEEK with and without the PEI insert were tested to ensure representative results. A vertical line was drawn on the sample sides 10 mm from the crack initiator in order to monitor crack growth. Test specimens were loaded at a constant displacement rate of 10 mm/min. Force and crosshead displacement were recorded during testing. This data was then used to calculate the energy, *A*, as per the standard [29] (Fig. 2).

The Mode I fracture toughness (*G_{Ic}*) was calculated using Eq. (1).

$$G_{Ic} = \frac{A}{a \times w} \times 10^6 \quad (1)$$

where *A* is the energy required to achieve the total propagated crack length, *a* is the propagated crack length and *w* is the specimen width.

3.1.2. Mode II interlaminar toughness

Mode II tests were carried out in accordance with AITM 1.0006 [32], which allows previously tested DCB specimens to be re-used to determine *G_{IIc}*. Tested DCB specimens were cut such that the pre-crack was 40 mm long. The specimens were placed across a 100 mm span, supported on 5 mm diameter rollers. The specimens were centrally loaded with a 10 mm diameter roller, with a 5 mm overhang on the pre-cracked end as illustrated in Fig. 3.

The specimens were loaded with a constant displacement rate of 1 mm/min. The Mode II interlaminar toughness (*G_{IIc}*) was found using Eq. (2).

$$G_{IIc} = \frac{9 \times P \times a^2 \times d \times 1000}{2 \times w \left(\frac{1}{4} L^3 + 3a^2 \right)} \quad (2)$$

where *P* is the critical load, *a* is the initial crack length, *d* is the deflection at the critical load, *w* is the specimen width and *L* is the span.

3.2. Impact testing

All panels were impacted by a drop-weight tower at different impact energies in accordance with ASTM Standard D7136 [31]. The impact tester was instrumented with a piezo-electric load-cell capable of measuring compressive forces up to 22kN. The velocity at impact, *v_i*, was determined by measuring the time the impactor took to pass between two laser sensors, spaced 60 mm apart immediately before the impact point. The panel was clamped onto a rigid base using four toggle clamps with rubber tips. In the machine, the 4.2 kg impactor is raised to the desired drop height using an electric winch motor. The drop height, *h*, is initially estimated by $h = E_{imp}/mg$, where *E_{imp}* is the impact energy, *m* is the mass of the impactor and *g* = 9.81 m/s². A pneumatic arm is employed to prevent the impactor from re-striking the test specimen if rebound occurs. Impact force as a function of time is recorded by the load-cell for each impact test. The bearing and guideline friction effect was neglected in the calculations.

All specimens were transversely impacted out-of-plane at the centre. Ultrasonic C-scan inspections were carried out to determine the internal damage of the post-impact laminates. C-scans were carried out using a TecScan C-Scanner with TecView analysing software, the gain of the machine during the test was 11 dB. Compression after impact (CAI) tests were carried out to determine

Table 1
Laminate description and corresponding stacking sequences.

Layup	Stacking Sequence	No. of Plies	Thickness (mm)	Nominal Fibre Volume Fraction (%)
ZD_NoFilm	[+45/90/-45/0 ₃ /+45/-45/0 ₃ /+45/90/-45/0 ₃ /-45/+45/0 ₃ /-45/90/+45]	25	4.65	66*
ZD_PEI	[+45/90/-45/PEI/0 ₃ /+45/PEI/-45/0 ₃ /PEI/+45/90/-45/PEI/0 ₃ /-45/PEI/+45/0 ₃ /PEI/-45/90/+45]	31	5.40	57*
ZD_PEEK	[+45/90/-45/PEEK/0 ₃ /+45/PEEK/-45/0 ₃ /PEEK/+45/90/-45/PEEK/0 ₃ /-45/PEEK/+45/0 ₃ /PEEK/-45/90/+45]	31	5.50	56*

* Fibre volume fraction values calculated using data from the Tenax®-E TPUD PEEK-2-34-IMS65 P12 24K-UD-190 product data sheet [26].

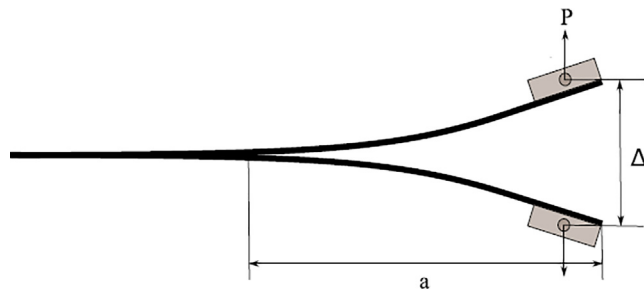


Fig. 2. DCB Schematic where P is the applied force, a is the crack length and Δ is the head displacement.

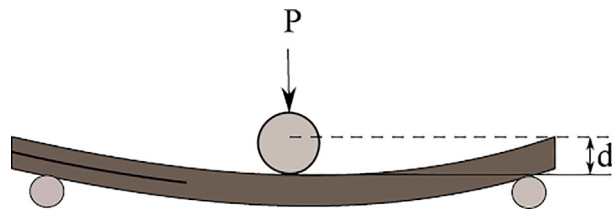


Fig. 3. ENF test – after test. Where d is the sample deflection at the critical load.

the residual strength of the panels post-impact. These tests were carried out according to ASTM D7137 [33] using an anti-buckling jig designed and manufactured according to the standard. The residual strength of each each layup at the three impacted energy levels looked at were compared to the undamaged compressive strength of these layups. The compressive strength of the undamaged specimens were found using a combined loading compression (CLC) test in accordance with ASTM D6641 [34]. The CLC test was used to determine the undamaged compressive strength of the different laminate types as the CAI test jig has been shown to demonstrate a relatively high incidence of undesirable failure modes such as end crushing in undamaged specimens [33]. While the compressive strength of a laminate can be influenced by the size of the specimen and the boundary conditions of the test [35], the CLC test yields valid undamaged compression strength values that can be used for comparison between the different laminate types. All CAI and CLC tests were carried out on a universal Zwick 300kN machine.

3.2.1. Calculations of dissipated energy

The energy dissipated by deformation mechanisms and damage during impact can simply be calculated by the kinematic equation according to Newton's second law of motion, provided by [31].

$$v(t) = v_i + gt - \int_0^t \frac{F(t)}{m} dt \tag{3}$$

where t is the current time during impact ($t = 0$ at the impact moment). $F(t)$ is the out-of-plane impact force introduced from the contact interaction between the impactor and the laminate, this

was measured using the impactor load-cell, and $v(t)$ is the corresponding velocity of the impactor. The velocity at impact, v_i , can be obtained from recording the time taken for the impactor to pass through two lasers mounted 60 mm apart as discussed in Section 3.2.

Displacement during impact, δ , was not measured experimentally, and was obtained from:

$$\delta(t) = \int_0^t v(t) dt = \delta_i + v_i t + \frac{gt^2}{2} - \int_0^t \left(\int_0^t \frac{F(t)}{m} dt \right) dt \tag{4}$$

With $\delta_i = 0$ as the initial displacement. Eq. (4) was also found to provide a reasonable trend of deformation during two phases of 'impact' and 'rebound', meaning that the maximum δ , is attained at the point where the velocity becomes zero. Dissipated energy is then obtained from the conservation of energy principle, and is given by:

$$E_a(t) = \frac{m(v_i^2 - v(t)^2)}{2} + mg\delta(t) \tag{5}$$

Terms $\int_0^t \frac{F(t)}{m} dt$ and $\int_0^t \left(\int_0^t \frac{F(t)}{m} dt \right) dt$ are numerically calculated as accumulative terms between the current and subsequent time steps. It is known that the total energy is absorbed when velocity becomes zero, and the deformation and damage mechanisms dissipate the initial kinetic energy introduced to the panel at the impact moment, i.e. $E_a^{max} = E_{imp}$, at $v = 0$.

Eq. (5) is used to obtain the evolution of dissipated energy during impact for each laminate and energy system, from the force data obtained experimentally. The results will be discussed in Section 4.2.

4. Results and discussion

4.1. Fracture toughness

4.1.1. Mode I

Both the baseline and PEI toughened CF/PEEK specimens displayed significant stick-slip. However, this was expected as Gao and Kim [8] determined that a high degree of crystallinity within CF/PEEK is a cause for stick-slip. For example, a 40% degree of crystallinity was achieved by Ray et al. [9] using a similar cooling rate. Stick-slip during testing was demonstrated by periods of steady crack growth followed by sudden, unstable crack growth. Upon carrying out visual inspections, stick-slip signs appeared as dark and light variations on the fracture surface as seen in Fig. 4. Colour variation correlated with the type of crack growth, with the lighter colour indicating stable crack growth, and dark indicating unstable crack growth [9].

The mixture of stable and unstable crack growth is likely caused by the variation in crystallinity throughout the sample. The PEI interleaf is miscible with PEEK, resulting in a hybrid blend of PEI/PEEK. As there is no control on how the PEI interacts with PEEK, variations between amorphous and crystalline resin regions occur throughout the laminate.



Fig. 4. Colour differences between stable and unstable crack growth (Note: the specimen is 25 mm wide).

Mode I interlaminar toughness values, calculated from the DCB test results (Fig. 5) using Eq. (1), are shown in Table 2. G_{Ic} values for PEI toughened CF/PEEK were 9.7% higher than baseline CF/PEEK. The baseline CF/PEEK energy release rate is lower than values found in literature [9], but a different grade of CF/PEEK was used in this study, i.e. the fibre type and polymer grade were different.

The large standard deviation for the thermoplastic specimens is attributed to the crack growth instability observed as a result of ductile and brittle crack propagation. Both laminate types exhibited unstable “jumps” in the crack length, and these unstable regions were not uniform in size. As the unstable growth was not uniform, the crack progressed differently through the width of the specimen, resulting in mixed mode fracture.

4.1.2. Mode II

The inclusion of PEI into the CF/PEEK mid-plane has a similar influence on Mode II interlaminar toughness as observed for Mode I interlaminar toughness. The G_{IIc} values are calculated using Eq. (2)

Table 2

DCB values for Mode I interlaminar toughness and standard deviation.

Laminate type	Propagation Energy Release Rate (J/m ²)	Standard Deviation (%)
Baseline CF/PEEK	992	10.8%
PEI toughened CF/PEEK	1088	10.9%

from the ENF results shown in Fig. 6. The G_{IIc} value for the baseline PEEK was determined to be 1767 J/m², with the PEI toughened CF/PEEK values being 31.3% higher at 2320 J/m² (Table 3). The G_{IIc} values for CF/PEEK are slightly higher than observed by Garcia Perez et al. [36], but a different grade of CF/PEEK was used in each study.

For Mode II fracture testing, it was observed that a higher force was required to propagate a crack within the PEI toughened CF/PEEK specimens. Similarly, the force for PEI toughened CF/PEEK specimens tended to plateau rather than decrease once the critical force was reached. The increase in displacement at a constant force value indicates higher energy is required to cause the crack to propagate within the toughened specimens. This was attributed to two mechanisms, firstly, more energy was required to stretch and rotate the amorphous chains within the specimen; secondly, the addition of the PEI interlayer increases the sample thickness, specifically increasing the resin rich mid-plane region. The large resin rich mid-plane encourages matrix deformation prior to crack growth, resulting in larger displacement prior to crack growth. The resin rich region is likely to allow for more matrix deformation prior to crack propagation, inducing the significantly greater toughness in the PEI toughened CF/PEEK specimens.

4.2. Evolution of impact force and absorbed energy

Fig. 7 shows representative force and energy absorption over time curves for 10 J impacts on both the toughened CF/PEEK (ZD_PEI and ZD_PEEK layups) and the baseline CF/PEEK panels (ZD layout). As shown in Fig. 7(a), the load/time curves for 10 J impacts show that the peak force for the PEI toughened panel (ZD_PEI) is 25% and 12% greater than for the baseline panel (ZD) and the PEEK insert panel (ZD_PEEK), respectively. The load/time curve also shows a relatively smooth impact loading/unloading

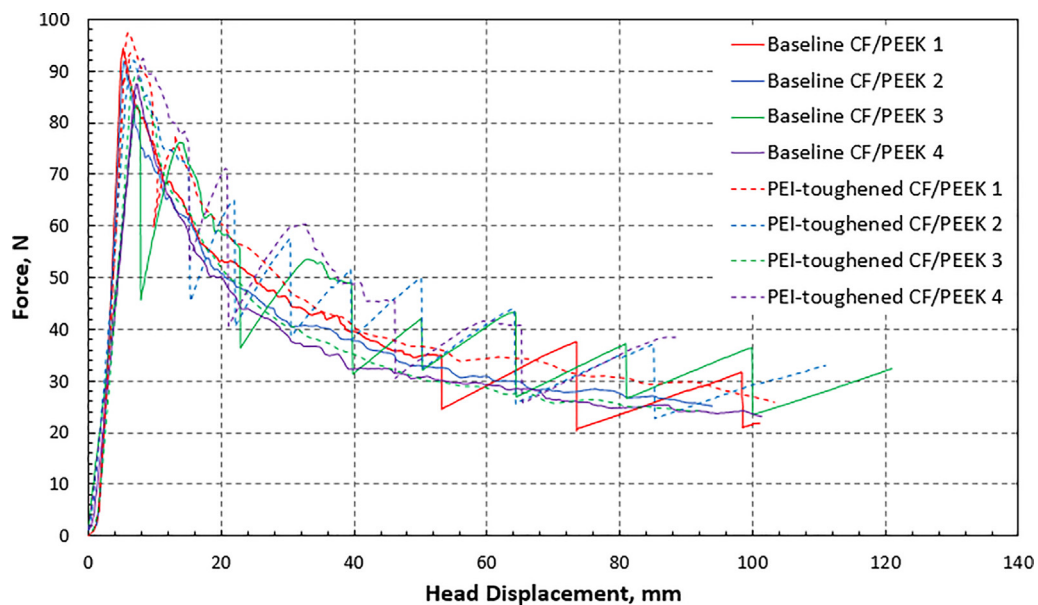


Fig. 5. Force vs displacement values found from DCB testing for baseline CF/PEEK and PEI toughened CF/PEEK specimens.

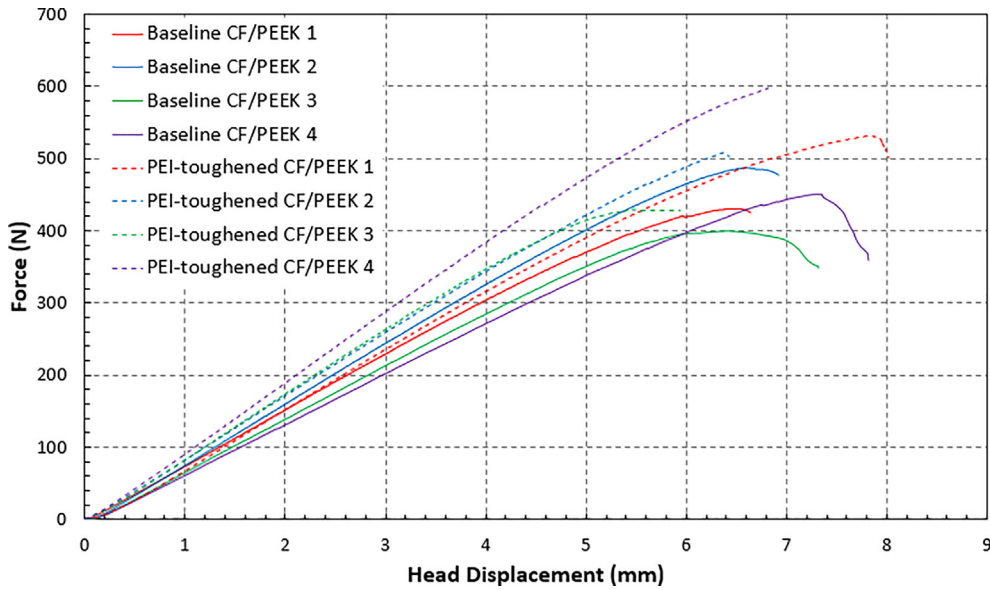


Fig. 6. Force vs displacement values found from ENF testing for baseline CF/PEEK and PEI toughened CF/PEEK specimens.

Table 3
ENF values for Mode II interlaminar toughness and standard deviation

Laminate Type	Energy Release Rate (J/m ²)	Standard Deviation (%)
Baseline CF/PEEK	1767	14.0%
PEI toughened CF/PEEK	2320	17.0%

behaviour for the PEI toughened panel at 10 J impact, whereas the baseline and PEEK insert panels exhibits a kink in the load/time curve at 6.76kN and 7.2kN respectively, indicating a significant damage event. From the absorbed energy vs time curves shown in Fig. 7(b), the residual energy of both the baseline and PEEK insert panels was around 2.9 J whereas the residual energy of the PEI toughened panel was 65% lower at a value of 1 J. This suggests that the added amorphous PEI layers help to toughen the panel, giving better impact performance compared to the baseline and PEEK insert panels.

Fig. 8 shows the results for panels subjected to a 20 J impact. All panel types experience kinks in the load/time curve, as shown in Fig. 8(a), indicating damage has occurred. The baseline panel (ZD layout) experiences a kink at 5.6kN before achieving a peak force of 8.86kN. The PEEK insert panel (ZD_PEEK layout) experiences a kink at 6.9kN before achieving a peak force of 9.7kN and the PEI toughened panel (ZD_PEI) experiences a kink at 8.2kN before achieving a peak force of 9.3kN. The PEI toughened panel was able to endure 46.4% more load than the baseline and 18.8% more load than the PEEK insert panel before experiencing the first signs of a damage event occurring. All panels then achieved relatively similar peak force, while there was also no significant difference between the absorbed energy curves, as shown in Fig. 8(b), although both insert panels (ZD_PEI and ZD_PEEK), had slightly lower residual energy than the baseline panel.

Fig. 9 shows the results for panels subjected to a 40 J impact. The baseline (ZD layout) panel's load/time curve indicates multiple damage events occurring. The first kink in the curve happens at a load of 6.4kN before reaching peak load of 14kN. The top of the

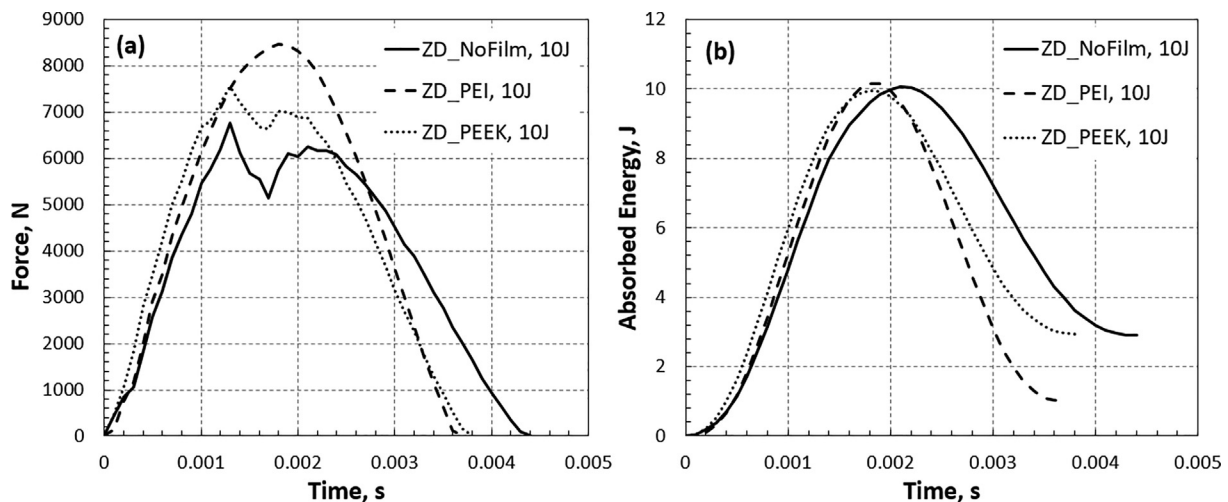


Fig. 7. Comparison of baseline and toughened panel's representative response to 10 J lateral impact energy; (a) evolution of impact force with time, and (b) absorbed energy with time.

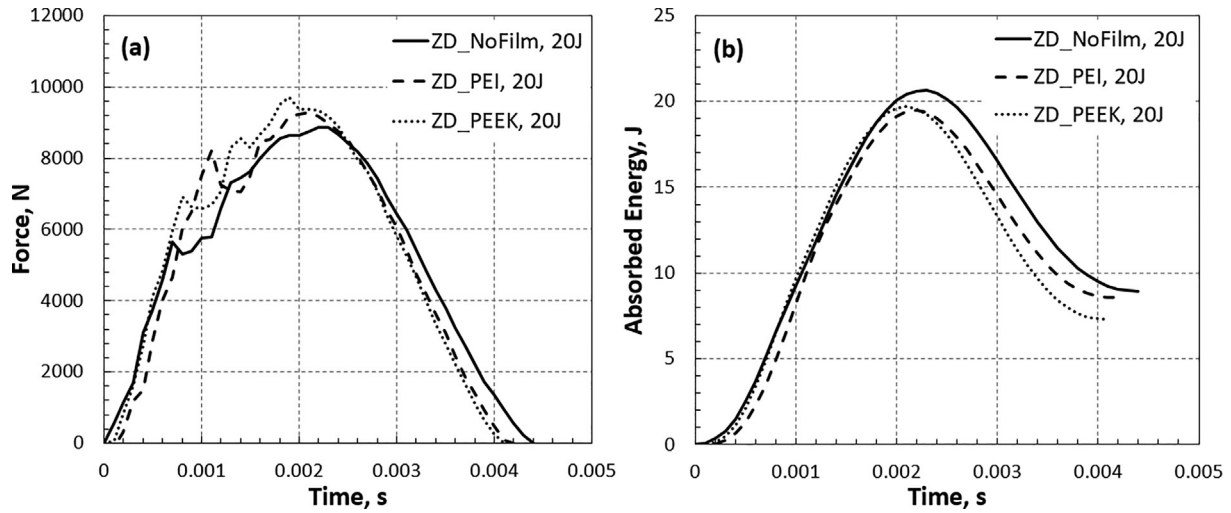


Fig. 8. Comparison of baseline and toughened panel's representative response to 20 J lateral impact energy; (a) evolution of impact force with time, and (b) absorbed energy with time.

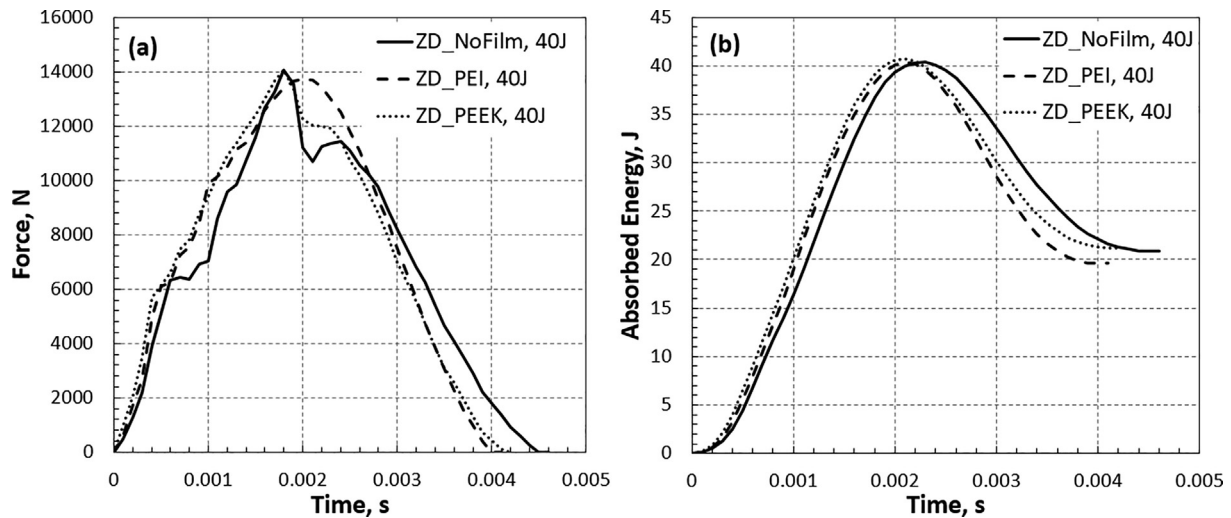


Fig. 9. Comparison of baseline and toughened panel's representative response to 40 J lateral impact energy; (a) evolution of impact force with time, and (b) absorbed energy with time.

load/time curve shows a significant reduction (23%), followed by a recovery of the load, indicating a major damage event. Contrary to the baseline panel, the two toughened panels have a relatively smooth load/time curve up until the peak force of 14kN is reached, at which point the PEEK insert panel (ZD_PEEK) experiences a sharp reduction in load (14%) before recovering slightly and following the same unloading path as both the baseline (ZD) and PEI toughened panel (ZD_PEI) to zero. The PEI toughened panel has a relatively smooth load/time curve with only small kinks in the curve at 6kN, 7.25kN and 9.8kN before reaching a peak of 14kN. Although a higher number of kinks are seen in the PEI toughened panels, they are substantially smaller damage events than those seen in the other two panels, which explains the slightly lower residual energy absorbed (19.6 J compared to 20.8 J in the other two panels – a 5.8% reduction) as shown in Fig. 9(b).

These results show that the initial damage event indicated by the first kink in the force time curve occurs at a higher load level in the PEI toughened panel than the baseline and PEEK insert panel at all three impact levels. The results suggest that the amorphous microstructure of the PEI plies increase the transverse toughness of the panel, compared to the more crystalline structure of the

baseline and PEEK insert panels. This agrees with the results obtained for Mode I and Mode II fracture toughness in presented in Section 4.1.

4.3. Damage area

4.3.1. Optical images

The optical images of the post-impact specimens—both impact surface and bottom surface—are shown in Figs. 10 and 11 for the 20 J and 40 J impact specimens, respectively. Images for the 10 J impacts are not presented, as the external observed damage was negligible. In Fig. 10, all 20 J impact specimen types clearly exhibit the indentation of the impactor in the centre of the panels along with cracks propagating from this point of impact. The top surface is a +45° ply, and the cracks can be seen to run both between (delamination) and across the fibres (fibre breakage) in the ply. These cracks are slightly larger on the PEI toughened panel compared to the other two panels. For the bottom side of the panels, there is a slight protusion, of equal size for all three panels, due to fibre breakout, typically associated with impact on composite laminates.

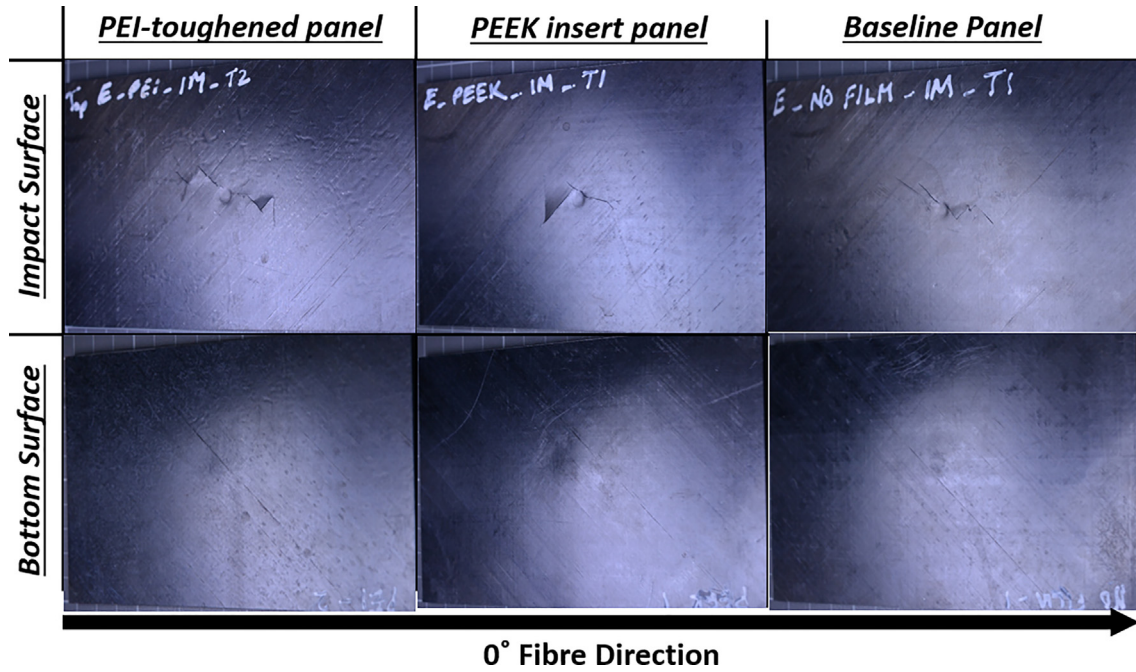


Fig. 10. Optical images of specimen impacted at 20 J.

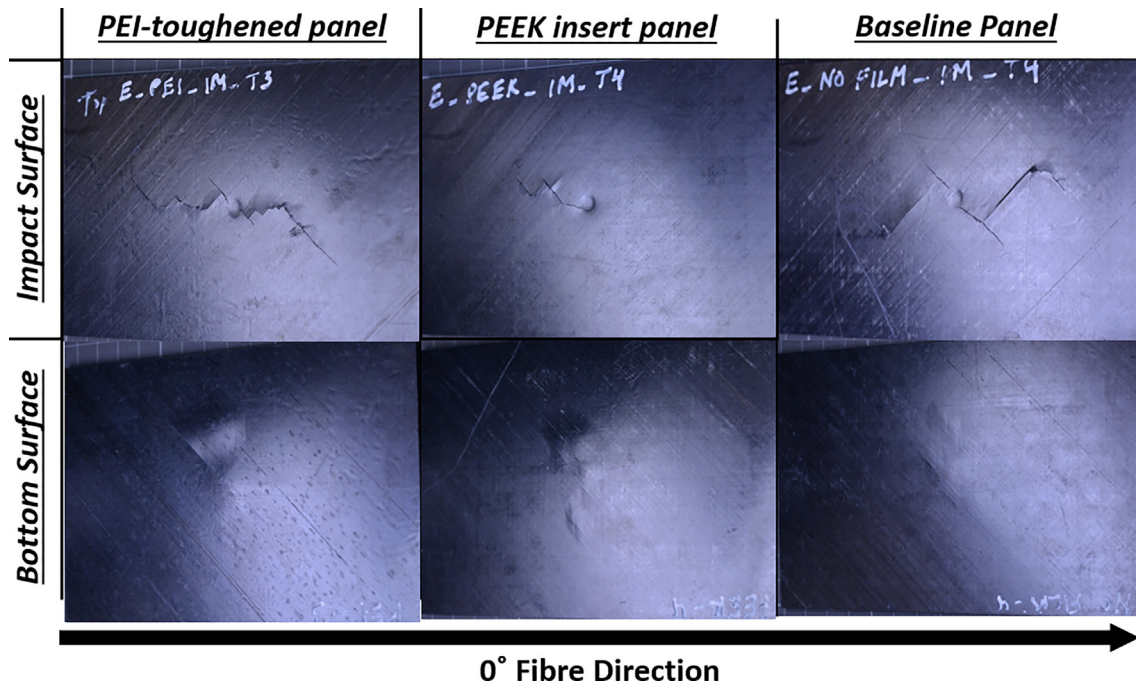


Fig. 11. Optical images of specimen impacted at 40 J.

The results of the 40 J impacts are shown in Fig. 11. As expected, the amount of damage exhibited on both the impact and bottom surface of the panels is increasing with the increasing impact energy levels. Again, cracks can be seen propagating from the point of impact on all three panels, with the largest cracks shown on the PEI toughened panel and baseline panel. The majority of cracks on the PEI toughened panel's impact surface are running across the fibres (fibre breakage) whereas the majority of cracks on the baseline panel are running along the fibres (matrix cracking and delamination). This results in cracks that extend mainly in the 0° (panel length) direction with slight radial growth for the PEI toughened

panel compared to the cracks on the baseline panel that shows more radial growth. The cracks on the PEEK insert panel run both across and along the fibres equally, however, the amount of cracks on this panel's surface is significantly lower than the other two panels. It should also be noted that the cracks propagate further from the point of impact on the PEI toughened panel when compared to the two other panels. Again, the bottom surface of all three specimens exhibit similar levels of protrusion due to fibre breakout.

It is worth noting that the damage exhibited by all panel types tested are at odds with the damage typically observed for fibre-

reinforced thermoset based composite laminates, where a small indent is generally observed on the top (impact) side, while significant 'break-out' in the form of delamination and fibre breakage is observed on the bottom side [4]. One hypothesis for this behaviour is that the tougher PEEK matrix acts as a buffer that dissipates and reflects the impact energy wave travelling through the laminate. For the laminates with PEI inserts, this phenomenon is magnified as the PEI inserts offer a more highly toughened layer. The reflected energy results in greater surface localised damage at the point of impact, while the dissipation of the energy wave travelling through the laminate results in less breakout damage on the bottom surface. An advantage of this phenomenon is that damage can be more easily detected as it appears on the impact surface, unlike in thermoset laminates where impact damage is barely visible on the surface, but significant damage exists internally.

4.3.2. C-scan images

Ultrasonic C-scan inspection images, presented in Figs. 12–14, were used to measure internal damage. Fig. 12 shows the damage caused in the panels for a 10 J impact event. As shown by Fig. 12(a), the damage in the PEI toughened panel is substantially smaller than the other 2 panels, 77% less than the PEEK insert panel and 82% less than the baseline panel. This correlates well with the load/time and absorption energy data presented in Fig. 7, which indicates that the baseline and PEEK insert panels experience more significant damage events than the PEI toughened panel.

Fig. 13 shows the damage caused in the panels for a 20 J impact event. Again, the damage footprint is smaller in the PEI toughened panel than the other 2 panels; 23% less than the PEEK insert panel and 21% less than the baseline panel.

Finally, Fig. 14 shows the damage caused in the panels for a 40 J impact event. As with the previous impact energies examined, the damage footprint in the PEI toughened panel is smaller than the other 2 panels; 34% less than the PEEK insert panel and 50% less than the baseline panel.

Damage in the panels grows radially with increasing energy, maintaining a semi-elliptical shape. The C-scan images show a combination of in-plane damage and delamination, separating the contributions of each damage type is not trivial. However, previous research has shown that the energy is predominantly absorbed by delamination mechanisms in carbon fibre thermosets panels (larger than 60% of the total energy) [4], which is presumed to be the dominant mechanism in terms of energy absorption behaviour in the panels examined in this study.

In all cases, the size of damage in the PEI toughened panels is smaller than that in the baseline and PEEK insert panels even though it appears that there is more damage visible on the impact surface of the PEI toughened panels. This indicates that the damage is spread more evenly throughout the layers of the PEI toughened

panel. This substantiates the assertion that adding amorphous PEI inserts enhance the damage resistance of CF/PEEK panels.

4.4. CAI results

Figs. 15–17 exhibit the CAI results for the panels impacted at 10 J, 20 J and 40 J. The results of panels that did not fail in the impact regions were not valid and removed from the data set. Each figure contains two parts: (a) the force–displacement results and (b) comparison of compressive residual strength with the results normalized to the PEI toughened panel. The compressive strength was obtained from the peak load divided by the panel width × thickness. Note that the PEEK insert panel (ZD_PEEK) is the thickest panel at 5.5 mm, followed by the PEI toughened panel (ZD_PEI) with a thickness of 5.4 mm followed by the baseline panel (ZD_NoFilm) at 4.65 mm.

Fig. 15 shows the results for the CAI tests for panels subjected to a 10 J impact. The PEEK insert panel did not fail in its impact region and its data was therefore removed. The PEI toughened panel reached a load level of 224kN before failure, 28.7% higher than the baseline panel failure load, 174kN. However, due to the baseline panel's lower thickness, its peak compressive strength was 9.8% lower than the PEI toughened panel.

Fig. 16 displays the results for the CAI tests for panels subjected to a 20 J impact. Again, the PEI toughened panel reached the highest compressive load before failing with a value of 194.4kN, followed by the PEEK insert panel with a value of 179kN and, finally, the baseline panel with a compressive failure load of 162.4kN. As shown in Fig. 17(b), the PEI toughened panel had the highest compressive residual strength, followed by the baseline panel which was around 10 MPa lower. The PEEK insert panel had the lowest compressive strength of the three panels impacted at 20 J.

Finally, Fig. 17 presents the results for the CAI tests for panels subjected to a 40 J impact. Fig. 17(a) indicates that the two modified panels fail at very similar load levels (around 160 kN) with the baseline panel failing at a much lower load (124.8 kN). Comparing compressive residual strength, there was minimal difference between the two modified panels, but the baseline panel had a significantly lower residual strength.

The results of the CAI tests indicate that the inclusion of amorphous PEI layers in the semi-crystalline CF/PEEK composite laminate improves its impact properties in terms of its residual strength.

4.5. CLC results

Table 4 shows the data collected for combined loading compression (CLC) testing of each of the laminate types. Two of the six PEI toughened specimens and three of the six PEEK insert spec-

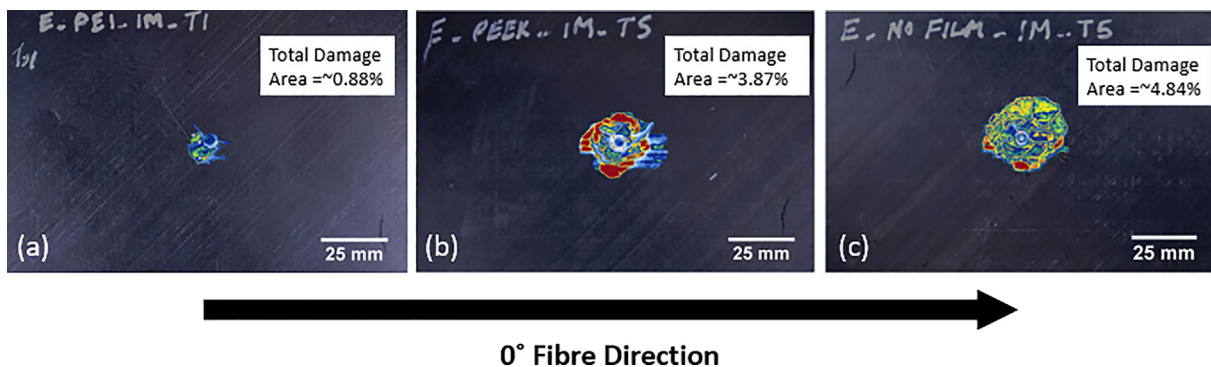


Fig. 12. Damage measured by C-scanning technique at 10 J impact energy level; (a) PEI toughened panel, (b) PEEK insert panel and (c) baseline panel.

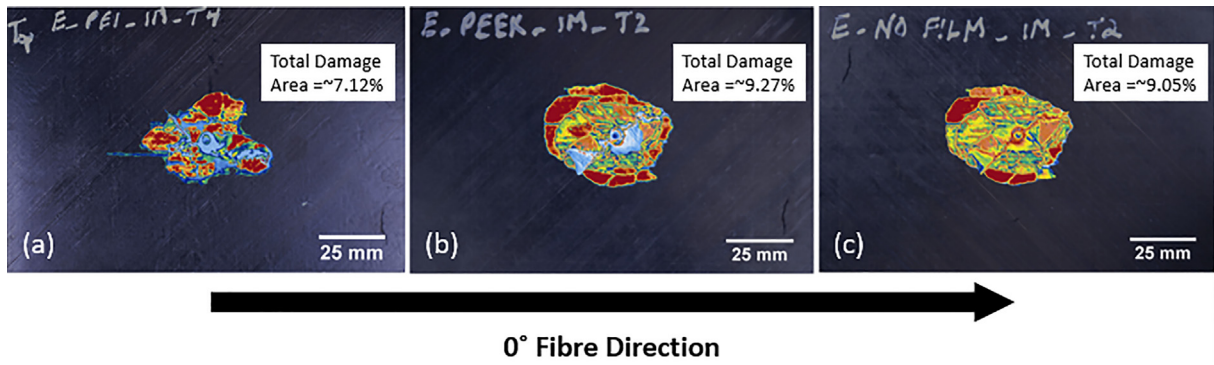


Fig. 13. Damage measured by C-scanning technique at 20 J impact energy level; (a) PEI toughened panel, (b) PEEK insert panel and (c) baseline panel.

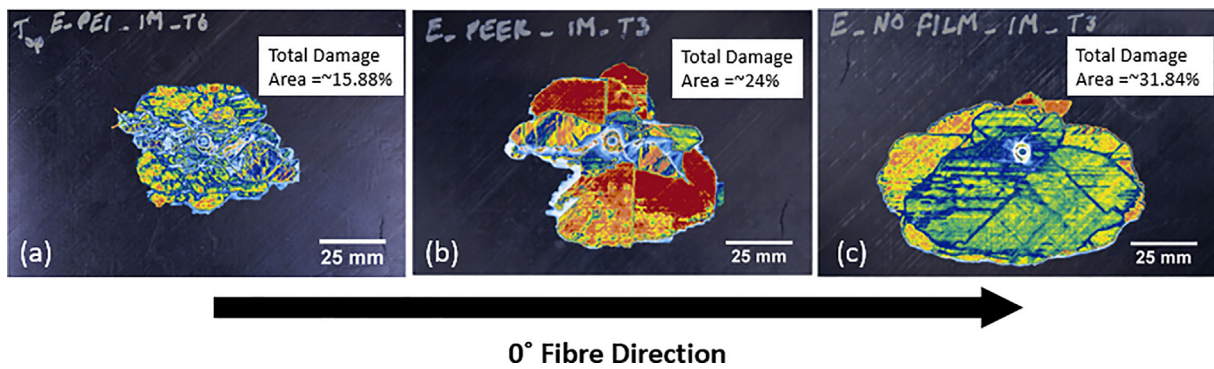


Fig. 14. Damage measured by C-scanning technique at 40 J impact energy level; (a) PEI toughened panel, (b) PEEK insert panel and (c) baseline panel.

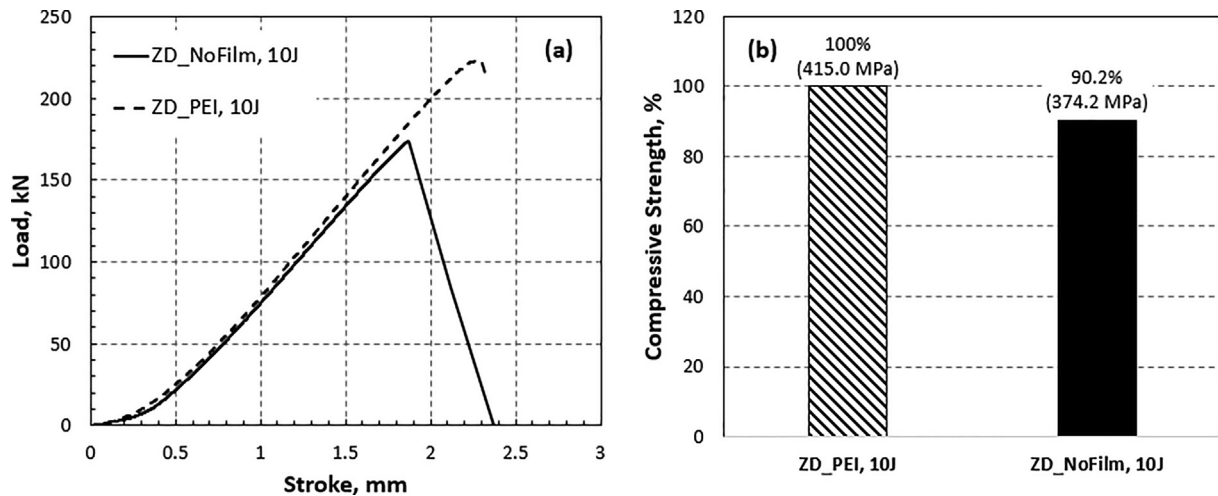


Fig. 15. Comparison of representative CAI results at 10 J – (a) Force-displacement results and (b) comparison of compressive residual strength.

imens broke in the grips of fixture, this failure was considered invalid and this data was discarded from the analysis.

The undamaged PEEK insert and baseline CLC specimens exhibited relatively higher strength prior to fracture compared to the PEI toughened panel. Fibre micro-buckling in the 0° fibres is the primary failure mechanism in a valid CLC specimen failure. The baseline laminate had a nominal fibre volume fraction of 66%, while the PEEK and PEI insert laminates had nominal fibre volume fractions of 56% and 57%, respectively. This reduction in fibre volume fraction is not evenly distributed throughout the laminate and is more acute in the plies adjacent to the PEI and PEEK film inserts, partic-

ularly the 0° plies. All laminates had equal numbers of 0° plies in the primary loading direction. The results suggest that lower local fibre volume fraction at the PEI and PEEK film interface plies may have had some influence on premature fibre bulking. In addition, the support provided by the local matrix also appears to have an influence on the fibre buckling. In the case of the PEI toughened panels, the amorphous PEI layers may provide less lateral support to the adjacent 0° plies, leading to fibre micro-buckling occurring at a lower compressive strength relative to the the baseline and PEEK insert specimens, where the semi-crystalline PEEK provides better lateral support.

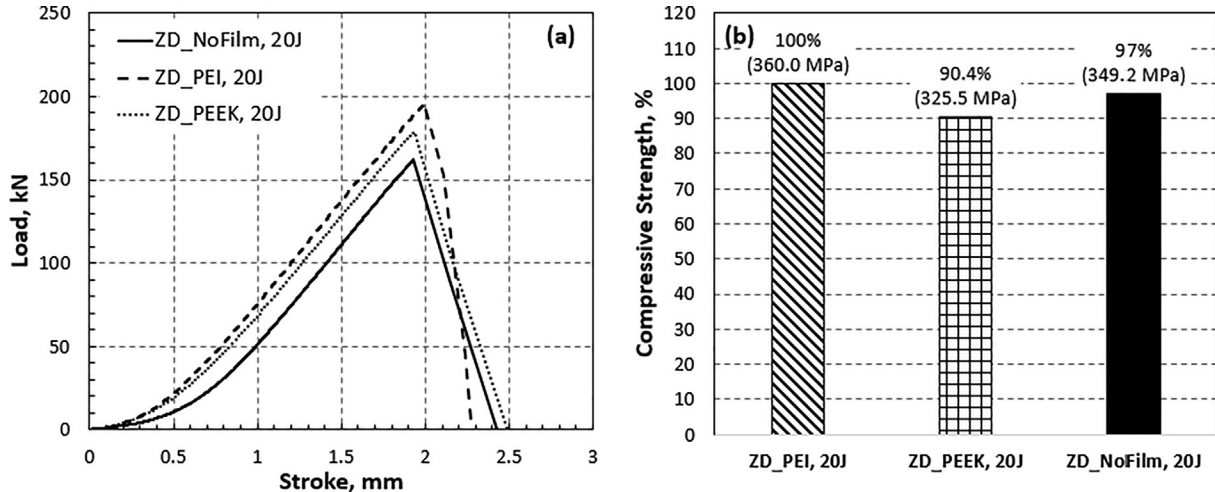


Fig. 16. Comparison of representative CAI results at 20 J – (a) Force-displacement results and (b) comparison of compressive residual strength.

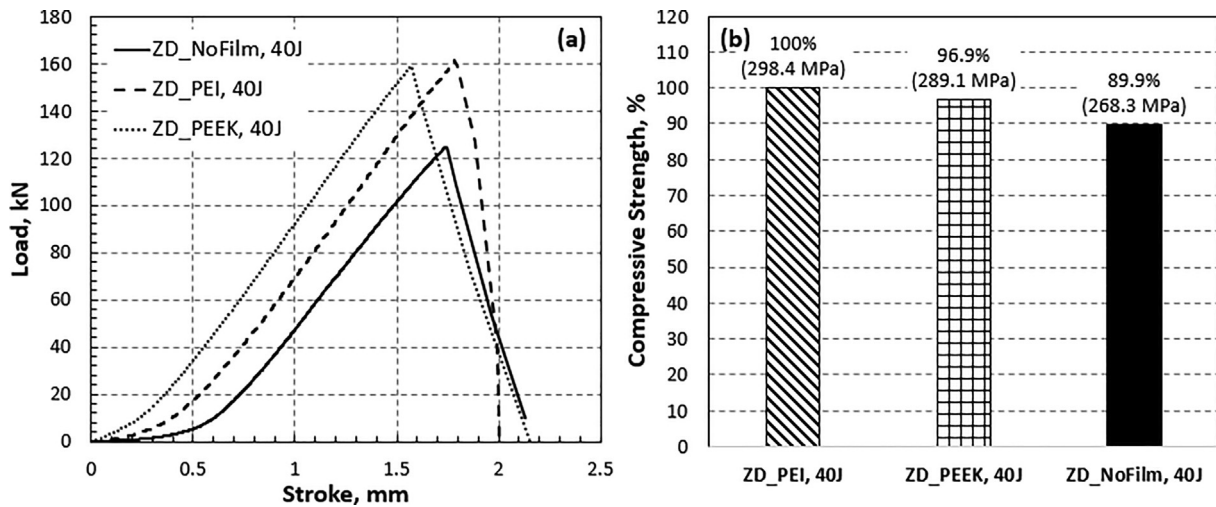


Fig. 17. Comparison of representative CAI results at 40 J – (a) Force-displacement results and (b) comparison of compressive residual strength.

Table 4
Results from CLC results on PEI toughened, PEEK insert and baseline specimens.

Specimen Number	ZD_PEI Compressive Strength (MPa)	ZD_PEEK Compressive Strength (MPa)	ZD_NoFilm Compressive Strength (MPa)
1	530.12	Specimen broke in grips	727.49
2	Specimen broke in grips	689.78	734.57
3	Specimen broke in grips	Specimen broke in grips	642.16
4	524.55	Specimen broke in grips	639.41
5	504.87	646.73	622.66
6	499.90	647.96	727.06
Average	514.86	661.50	682.22

4.6. Residual strength

The results from the CAI tests (residual compressive strength of the damaged specimens) are compared to the CLC tests results (compressive strength of the undamaged specimens) to assess the damage tolerance of each of the laminate types. While the CAI and CLC specimens are not the same size and are not subjected

to the same boundary conditions during testing, in this study they can provide data for relative comparison of different laminate types, rather than giving quantitative values for laminate damage tolerance. Fig. 18 indicates that although the PEEK insert and baseline specimens have a larger undamaged compressive strength than the PEI toughened specimens, the damaged PEI toughened specimens have the greater relative residual strength for all the impact energies analysed. Although there is a trade-off when it comes to undamaged compressive strength, the PEI toughened specimens exhibit greater damage tolerance compared to the PEEK insert specimens and baseline PEEK specimens.

This can be seen more clearly when the data is normalised as a percentage of the undamaged compressive strength as shown in Fig. 19. For the PEI toughened specimens, 79% of the undamaged strength was retained at 10 J impact, compared to 57% for the baseline PEEK specimen and 49% for the PEEK insert specimen. 69% of the undamaged strength was retained at 20 J impacts for the PEI toughened specimens when compared to roughly 50% for the PEEK insert and baseline specimens. For a 40 J impact, 57% of the undamaged strength was retained for the PEI toughened specimens compared to 41% for the baseline PEEK specimens and 44% for the PEEK insert specimens. Considering that structural buckling behaviour

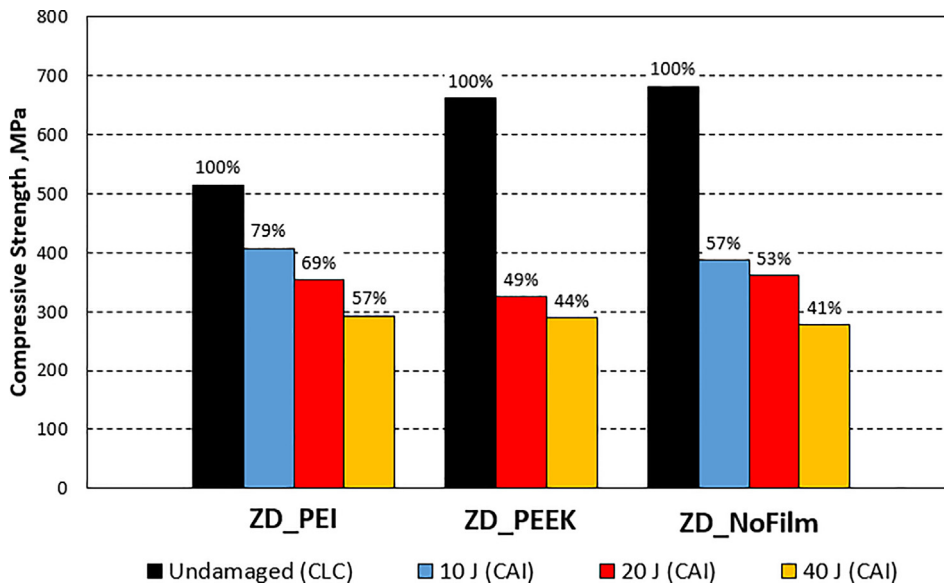


Fig. 18. Undamaged strength (obtained from CLC testing) vs residual strength (obtained from CAI testing) – Actual Data.

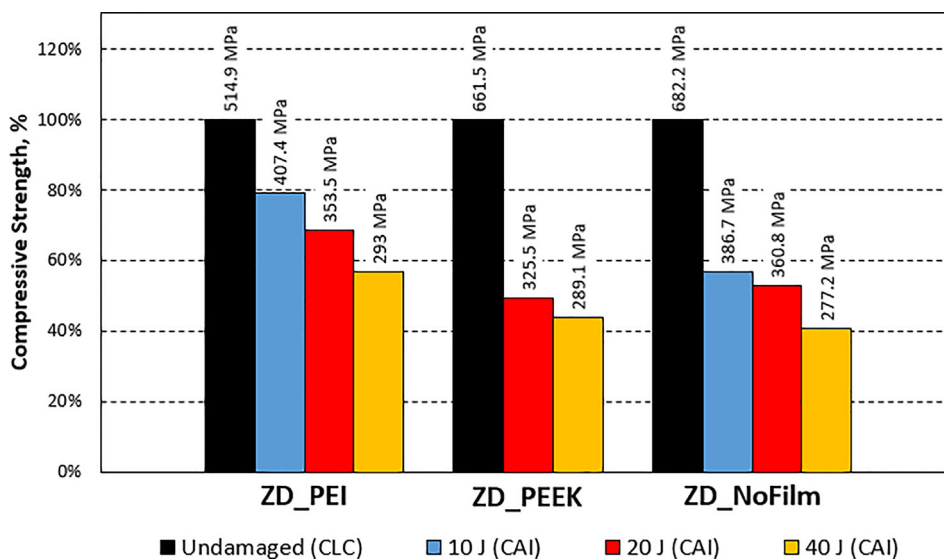


Fig. 19. Undamaged strength (obtained from CLC testing) vs residual strength (obtained from CAI testing) – Normalised data.

and compressive residual strength after impact are generally greater design considerations in aircraft design, rather than pure material compressive strength [37,38], this work presents interesting data for design of CF/PEEK aircraft structures.

5. Conclusions

In this study, the effect of using amorphous PEI inserts on the toughness and the impact damage resistance of CF/PEEK laminates was investigated. To the authors' best knowledge, this is the first time that a study of the influence of PEI inserts on the toughness of CF/PEEK laminates has been presented in the open literature. While the influence of processing parameters on toughness of CF/PEEK laminates has been studied previously [7–12] and the influence of PEI and other coatings on the fibre/matrix interface in CF/PEEK has been investigated [13–20], the method outlined herein builds on the knowledge developed by these researchers, but offers a different approach to localised interlaminar toughening. It was

found that the inclusion of a PEI layer increased the Mode I interlaminar toughness by 9.7%, while the Mode II interlaminar toughness increased by 17.9%. The scatter associated with the Mode II interlaminar toughness data is attributed to the crack growth instability observed as a result of ductile and brittle crack propagation. Similarly, both thermoplastic sample groups displayed “stick-slip” during Mode I testing, indicating a high degree of crystallinity [8] in both sample groups. Stick-slip was more prominent in the toughened specimens, this was attributed to the variations in the crystallinity of the PEI/PEEK hybrid polymer interlayer at the laminate mid-plane. The fracture surfaces of the PEI toughened PEEK specimens indicate regions within each specimen that display signs of amorphous deformation, highlighting that the PEI/PEEK blend is non-uniform throughout the sample. The results found in this interlaminar toughness study supported the use of PEI film inserts as a toughening mechanism for impact damage of thermoplastic laminates. In particular, the higher Mode II toughness should yield a higher impact damage resistance.

The low-velocity impact response of a baseline and two modified types of CF/PEEK laminate was investigated. Drop-weight impact test curves, C-scans of impact damage and CAI compressive residual strength data were analysed to compare the laminate responses. The study showed that the PEI toughened panel performed better than both the baseline panel and the PEEK insert panel, especially at lower impact energy levels (10 J) associated with drop tool impact events. Damage associated with low velocity drop tool impact and airport ramp activity are a key design consideration. The PEI toughened panels are less susceptible to this type of damage event. Even at a higher impact energy (20 J), there was a delay in the first damage event occurring for the PEI toughened panel compared to the other two panels. C-scan images indicate that the addition of the amorphous PEI layer has provided an enhancement in the impact damage response of the CF/PEEK laminate, the relative footprint size of the damage zone is smaller and the damage appears to be spread more evenly through all layers of the laminate. The relatively smaller damage footprint improved the CAI residual strength of the laminate at lower impact energy levels. Interestingly, all specimens exhibited significant cracking on the impact surface of the laminates, unlike what is commonly observed in thermoset based composite laminate structures. From an in-service maintenance perspective, this is very useful as the point of impact and associated damage are obvious on the surface of the laminate allowing damaged structure to be easily identified and appropriate maintenance to be carried out.

When comparing the residual CAI strength to the undamaged compressive strength obtained from the CLC test, it was found that the PEI toughened specimens were able to retain a much higher percentage of the panels undamaged strength at all energy levels when compared to the PEEK insert and baseline CF/PEEK laminates. There is a trade-off, as the PEI toughened laminate's undamaged strength is around 25% lower than the PEEK-only specimens, most likely due to the lower buckling resistance provided by the amorphous PEI layers. However, the CAI strength of the PEI toughened sample was still greater than the CF/PEEK baseline specimens, especially at the 10 J and 20 J impact energies, even with its lower undamaged compressive strength.

The data obtained during this study indicates that a PEI toughened CF/PEEK hybrid laminate could be used in structures that are vulnerable to impact events to provide greater impact damage resistance and damage tolerance.

Declaration of Competing Interest

The authors declare that they have no known competing financial interests or personal relationships that could have appeared to influence the work reported in this paper.

Acknowledgements

This research was supported by the funding from the Irish Research Council (IRC) under the Government of Ireland Postgraduate Scholarship Programme (GOIPG/2018/2439).

References

- [1] C.A. Wenner, C.G. Drury, Analyzing human error in aircraft ground damage incidents, *Int. J. Ind. Ergon.* 26 (2) (2000) 177–199, [https://doi.org/10.1016/S0169-8141\(99\)00065-7](https://doi.org/10.1016/S0169-8141(99)00065-7).
- [2] E.V. González, P. Maimí, P.P. Camanho, A. Turon, J.A. Mayugo, Simulation of drop-weight impact and compression after impact tests on composite laminates, *Compos. Struct.* 94 (11) (2012) 3364–3378, <https://doi.org/10.1016/j.compstruct.2012.05.015>.
- [3] Y. Shi, T. Swait, C. Soutis, Modelling damage evolution in composite laminates subjected to low velocity impact, *Compos. Struct.* 94 (9) (2012) 2902–2913, <https://doi.org/10.1016/j.compstruct.2012.03.039>.
- [4] H. Yazdani Nezhad, F. Merwick, R.M. Frizzell, C.T. McCarthy, Numerical analysis of low-velocity rigid-body impact response of composite panels, *Int. J. Crashworthiness* 20 (1) (2015) 27–43, <https://doi.org/10.1080/13588265.2014.963378>.
- [5] W.J. Cantwell, J. Morton, The impact resistance of composite materials – a review, *Composites* 22 (5) (1991) 347–362, [https://doi.org/10.1016/0010-4361\(91\)90549-V](https://doi.org/10.1016/0010-4361(91)90549-V).
- [6] S. Abrate, Impact on Laminated Composite Materials, *Appl. Mech. Rev.* 44 (4) (1991) 155–190, <https://doi.org/10.1115/1.3119500>.
- [7] S.-L. Gao, J.-K. Kim, Cooling rate influences in carbon fibre/PEEK composites. Part I: Crystallinity and interface adhesion, *Compos. Part A Appl. Sci. Manuf.* 31 (6) (2000) 517–530, [https://doi.org/10.1016/S1359-835X\(00\)00009-9](https://doi.org/10.1016/S1359-835X(00)00009-9).
- [8] S.-L. Gao, J.-K. Kim, Cooling rate influences in carbon fibre/PEEK composites. Part II: interlaminar fracture toughness, *Compos. Part A Appl. Sci. Manuf.* 32 (6) (2001) 763–774, [https://doi.org/10.1016/S1359-835X\(00\)00188-3](https://doi.org/10.1016/S1359-835X(00)00188-3).
- [9] D. Ray, A.J. Comer, J. Lyons, W. Obande, D. Jones, R.M.O. Higgins, M.A. McCarthy, Fracture toughness of carbon fiber/polyether ether ketone composites manufactured by autoclave and laser-assisted automated tape placement, *J. Appl. Polym. Sci.* 132 (11) (2014) 1–10, <https://doi.org/10.1002/app.41643>.
- [10] A.J. Comer, D. Ray, W.O. Obande, D. Jones, J. Lyons, I. Rosca, R.M. O' Higgins, M. A. McCarthy, Mechanical characterisation of carbon fibre-PEEK manufactured by laser-assisted automated-tape-placement and autoclave, *Compos. Part A Appl. Sci. Manuf.* 69 (2015) 10–20, <https://doi.org/10.1016/j.compositesa.2014.10.003>.
- [11] F. Shadmehri, S.V. Hoa, J. Fortin-Simpson, H. Ghayoor, Effect of in situ treatment on the quality of flat thermoplastic composite plates made by automated fiber placement (AFP), *Adv. Manuf. Polym. Compos. Sci.* 4 (2) (2018) 41–47, <https://doi.org/10.1080/20550340.2018.1444535>.
- [12] A. Chanteli, A.K. Bandaru, D. Peeters, R.M. O'Higgins, P.M. Weaver, Influence of repair treatment on carbon fibre-reinforced PEEK composites manufactured using laser-assisted automatic tape placement, *Compos. Struct.* 248 (May 2020) (2020), <https://doi.org/10.1016/j.compstruct.2020.112539>.
- [13] M. He, X. Chen, Z. Guo, X. Qiu, Y. Yang, C. Su, N. Jiang, Y. Li, D. Sun, L. Zhang, Super tough graphene oxide reinforced polyetheretherketone for potential hard tissue repair applications, *Compos. Sci. Technol.* 174 (March) (2019) 194–201, <https://doi.org/10.1016/j.compscitech.2019.02.028>.
- [14] S.L. Chuang, N.-J. Chu, W.T. Whang, Effect of polyamic acids on interfacial shear strength in carbon fiber/aromatic thermoplastics, *J. Appl. Polym. Sci.* 41 (12) (1990) 373–382, <https://doi.org/10.1002/app.1990.070410129>.
- [15] N. Li, L. Zong, Z. Wu, C. Liu, X. Wang, F. Bao, J. Wang, X. Jian, Amino-terminated nitrogen-rich layer to improve the interlaminar shear strength between carbon fiber and a thermoplastic matrix, *Compos. Part A Appl. Sci. Manuf.* 101 (2017) 490–499, <https://doi.org/10.1016/j.compositesa.2017.06.023>.
- [16] N. Li, Z. Wu, L. Huo, L. Zong, Y. Guo, J. Wang, X. Jian, One-step functionalization of carbon fiber using in situ generated aromatic diazonium salts to enhance adhesion with PPBES resins, *RSC Adv.* 6 (74) (2016) 70704–70714, <https://doi.org/10.1039/c6ra12717g>.
- [17] H. Yuan, S. Zhang, C. Lu, S. He, F. An, Improved interfacial adhesion in carbon fiber/polyether sulfone composites through an organic solvent-free polyamic acid sizing, *Appl. Surf. Sci.* 279 (2013) 279–284, <https://doi.org/10.1016/j.apsusc.2013.04.085>.
- [18] L. WenBo, Z. Shu, H. LiFeng, J. WeiCheng, Y. Fan, L. Li. XiaoFei, W. RongGuo, Interfacial shear strength in carbon fiber-reinforced poly(phthalazinone ether ketone) composites, *Polym. Compos.* 34 (11) (2013) 1921–1926, <https://doi.org/10.1002/pc.22599>.
- [19] J. Li, Interfacial studies on the ozone and air-oxidation-modified carbon fiber reinforced PEEK composites, *Surf. Interface Anal.* 41 (4) (2009) 310–315, <https://doi.org/10.1002/sia.v41:410.1002/sia.3023>.
- [20] J. Chen, K. Wang, Y. Zhao, Enhanced interfacial interactions of carbon fiber reinforced PEEK composites by regulating PEI and graphene oxide complex sizing at the interface, *Compos. Sci. Technol.* 154 (2018) 175–186, <https://doi.org/10.1016/j.compscitech.2017.11.005>.
- [21] H. Yun, F.-K. Chang, A Model for Predicting Damage in Graphite/Epoxy Laminated Composites Resulting from Low-Velocity Point Impact, *J. Compos. Mater.* 26 (14) (1992) 2134–2169, <https://doi.org/10.1177/002199839202601408>.
- [22] G. Clark, Modelling of impact damage in composite laminates, *Composites* 20 (3) (1989) 209–214, [https://doi.org/10.1016/0010-4361\(89\)90335-2](https://doi.org/10.1016/0010-4361(89)90335-2).
- [23] H.R. Wang, S.C. Long, X.Q. Zhang, X.H. Yao, Study on the delamination behavior of thick composite laminates under low-energy impact, *Compos. Struct.* 184 (September 2017) (2018) 461–473, <https://doi.org/10.1016/j.compstruct.2017.09.083>.
- [24] G.W. Ehrenstein, *Polymeric Materials: Structure, Properties, Applications*, Hanser, Munich, 2001.
- [25] S. Carroccio, C. Puglisi, G. Montaudo, Thermal degradation mechanisms of polyetherimide investigated by direct pyrolysis mass spectrometry, *Macromol. Chem. Phys.* 200 (10) (1999) 2345–2355, [https://doi.org/10.1002/\(SICI\)1521-3935\(19991001\)200:10<2345::AID-MACP2345>3.0.CO;2-T](https://doi.org/10.1002/(SICI)1521-3935(19991001)200:10<2345::AID-MACP2345>3.0.CO;2-T).
- [26] Teijin, "Tenax®-E TPU PEEK-IMS65 Material Data Sheet." pp. 1–2, 2019. doi: 10.1002/9781118785317.weom080108.
- [27] K.H. Oh, Y.-H. Ko, K.-J. Kim, Mechanical properties of amorphous PEI, PES, and PVC up to 11 GPa studied by Brillouin light scattering, *Phys. B Condens. Matter* 576 (2020), <https://doi.org/10.1016/j.physb.2019.411722>.
- [28] F.N. Cogswell, *Thermoplastic Aromatic Polymer Composites*, Butterworth-Heinemann Ltd., Oxford, 1992. 10.1533/9781845699253.

- [29] A. Industrie, AITM 1.0005: Carbon Fiber Reinforced Plastics – Determination of Interlaminar Fracture Toughness Energy Mode I – TEST, Airbus Industrie, Blagnac, 1994.
- [30] P.J. Gray, R.M. O'Higgins, C.T. McCarthy, Effects of laminate thickness, tapering and missing fasteners on the mechanical behaviour of single-lap, multi-bolt, countersunk composite joints, *Compos. Struct.* 107 (1) (2014) 219–230, <https://doi.org/10.1016/j.compstruct.2013.07.017>.
- [31] ASTM D7136/D7136M-20: Standard Test Method for Measuring the Damage Resistance of a Fiber-Reinforced Polymer Matrix Composite to a Drop-Weight Impact Event, ASTM International, West Conshohocken, PA, 2020. doi: [10.1520/D7136_D7136M-20](https://doi.org/10.1520/D7136_D7136M-20).
- [32] A. Industrie, AITM 1.0006: Carbon Fiber Reinforced Plastics – Determination of Interlaminar Fracture Toughness Energy Mode II – TEST, Airbus Industrie, Blagnac, 1994.
- [33] ASTM D7137/D7137M-17: Standard Test Method for Compressive Residual Strength Properties of Damaged Polymer Matrix Composite Plates. ASTM International, West Conshohocken, PA, 2017. doi: [10.1520/D7137_D7137M-17](https://doi.org/10.1520/D7137_D7137M-17).
- [34] ASTM D6641/D6641M-16e2: Standard Test Method for Compressive Properties of Polymer Matrix Composite Materials Using a Combined Loading Compression (CLC) Test Fixture, ASTM International, West Conshohocken, PA, 2016. doi: [10.1520/D6641](https://doi.org/10.1520/D6641).
- [35] P.G. Slattery, C.T. McCarthy, R.M. O'Higgins, Assessment of residual strength of repaired solid laminate composite materials through mechanical testing, *Compos. Struct.* 147 (2016) 122–130, <https://doi.org/10.1016/j.compstruct.2016.03.036>.
- [36] P. Garcia Perez, C. Bouvet, A. Chettah, F. Dau, L. Ballere, P. Pèrès, Effect of unstable crack growth on mode II interlaminar fracture toughness of a thermoplastic PEEK composite, *Eng. Fract. Mech.* 205 (2019) 486–497, <https://doi.org/10.1016/j.engfracmech.2018.11.022>.
- [37] R.R. Boyer, J.D. Cotton, M. Mohaghegh, R.E. Schafrik, Materials considerations for aerospace applications, *MRS Bull.* 40 (12) (2015) 1055–1066, <https://doi.org/10.1557/mrs.2015.278>.
- [38] T.H.G. Megson, *Aircraft Structures for Engineering Students*, 3rd ed. London, 1972.